

MULTIMODAL IMAGING OF MULTIFOCAL CHOROIDITIS WITH ADAPTIVE OPTICS OPHTHALMOSCOPY

Sohani Amarasekera, MD,* Andrew M. Williams, MD,* K. Bailey Freund, MD,†‡
Ethan A. Rossi, PhD,*§ Kunal K. Dansingani, MA, FRCOphth*

Purpose: To describe longitudinal, anatomical, and functional alterations caused by inflammatory and neovascular lesions of idiopathic multifocal choroiditis/punctate inner choroidopathy using adaptive optics imaging and microperimetry.

Methods: Longitudinal case study using multiple imaging modalities, including spectral-domain optical coherence tomography, fluorescein angiography, indocyanine green angiography, optical coherence tomography angiography, flood illumination adaptive optics, and microperimetry.

Results: A 21-year-old myopic Asian man presented with blurred vision in the right eye. Clinical examination was notable for an isolated hypopigmented, perifoveal lesion in each eye. Multimodal imaging showed inflammatory lesions in the outer retina, retina pigment epithelium, and inner choroid lesions of both eyes. The right eye additionally exhibited active Type-2 macular neovascularization with loss of cone mosaic regularity that was associated with reduced sensitivity on microperimetry. The clinical picture was consistent with multifocal choroiditis/punctate inner choroidopathy. The patient was treated with oral steroids and three injections of intravitreal bevacizumab in the right eye. After therapy, imaging showed reestablishment of the cone mosaic on flood illumination adaptive optics and improvement in sensitivity on microperimetry.

Conclusion: Adaptive optics imaging and microperimetry may detect biomarkers that help to characterize the nature and activity of multifocal choroiditis lesions and to help monitor response to therapy. With timely intervention, structural abnormalities in the outer retina and choroid can be treated, and anatomical improvements precede improvements in visual function.

RETINAL CASES & BRIEF REPORTS 16:747–753, 2022

*From the *Department of Ophthalmology, Eye and Ear Institute, University of Pittsburgh Medical Center, Pittsburgh, Pennsylvania; †Vitreous Retina Macular Consultants of New York, New York, New York; ‡LuEsther T. Merz Retinal Research Center, Manhattan Eye, Ear and Throat Hospital, New York, New York; and §Department of Bioengineering, Swanson School of Engineering, University of Pittsburgh, Pittsburgh, Pennsylvania.*

Idiopathic multifocal choroiditis (MFC) is an inflammatory syndrome considered to be on the same spectrum as punctate inner choroidopathy. Pathologic changes occur at the level of the outer retina, retinal pigment epithelium (RPE), and choriocapillaris.¹ In addition to inflammatory lesions asso-

ciated with the disease, up to 60% of cases can be complicated by the development of macular neovascularization (NV), frequently with a Type-2 configuration.^{2,3} Appropriate management of MFC is dependent upon accurate determination of the type and activity of MFC lesions. Advances in imaging can aid in both diagnosing and characterizing MFC lesions and in assessing response to therapeutic intervention.

Herein, we present a case of MFC and report the findings of multimodal imaging, including spectral-domain optical coherence tomography (OCT; Spectralis, Heidelberg Engineering, Germany), OCT angiography (RTVue XR 100 Avanti Edition; Optovue, Fremont, CA), commercially available flood-illumination adaptive optics (FIAO), retinal camera (rtx1, Imagine Eyes, Orsay, France), and confocal

microperimetry, from initial presentation to nine months of follow-up. The purpose of this article was to provide a longitudinal study of the anatomical and functional alterations associated with inflammatory and neovascular MFC lesions using adaptive optics imaging and microperimetry and to illustrate how these pathologic changes respond to appropriate therapy.

Case Report

A 21-year-old myopic (−3.00 diopters) Asian man without ocular or medical history presented to the retina service with a 2-day history of blurred vision in the right eye. Visual acuity was 20/40 in the right eye, with pinhole improvement to 20/30, and 20/40 in the left eye with pinhole improvement to 20/25. Anterior segment examination was unremarkable, with neither cell nor flare in either eye. Ophthalmoscopy of the right eye was notable for vitritis and a hypopigmented lesion at the superonasal border of the fovea. The left eye did not exhibit vitreous inflammation, but examination was notable for a hypopigmented lesion temporal to the fovea (Figure 1, top row).

Optical coherence tomography through the fovea of the right eye revealed a focal area of hyperreflective material, splitting of the RPE/Bruch membrane complex with overlying subretinal hyperreflective material, ellipsoid zone and interdigitation zone disruption, and hypertransmission into the choroid. Optical coherence tomography of the left macula revealed a hypertransmissive atrophic lesion, minimal subretinal hyperreflective material, and choroidal thickening, suggestive of prior inflammation (Figure 1, middle row). There was no cystoid macular edema in either eye. Fluorescein angiography demonstrated early focal hyperfluorescence with late leakage in the right eye, suggestive of Type-2 macular NV and midphase hyperfluorescence without leakage in the left eye (Figure 1, third row). Indocyanine green angiography in both eyes demonstrated hypofluorescence of the lesions, attributed to loss of fluorescence from the inner choroid (Figure 1, third row). A flow signal was detected in the lesion in the right eye by OCT angiography, segmented at the level of the outer retina and choriocapillaris (Figure 1, fourth row).

Adaptive optics images were obtained, and a montage was generated for each eye. In the right eye, there was loss of cone visibility near the fovea with a surrounding rim of patchy regularity in the cone mosaic that was then circumscribed by a larger area of loss of visible cones, particularly superonasally and inferior to the fovea (Figure 2). It should be noted that the FIAO device used here

lacks the resolution to image the smallest foveal cones, so cones within 1 to 2 degrees of the foveal center could not be assessed. The cone photoreceptors were otherwise uniformly dense and regularly arranged in the right macula. In the left eye, the cone mosaic was generally preserved, but there was a lesion temporal to the fovea that demonstrated loss of visible cones centrally with a central hyperreflectivity surrounded by a hyporeflexive halo. Baseline microperimetry in the right eye showed stable fixation with an average threshold sensitivity of 26.8 decibels (dB). This reduction in average threshold represented less than the fifth percentile compared with age-matched controls. In addition to this generalized reduction in sensitivity, there was also localized reduction in macular sensitivity threshold at the loci tested in the superior and superonasal perifoveal regions (15 dB) at the location of the choroidal lesion. Similar microperimetry findings were demonstrated at baseline in the left eye with stable fixation, but with a generalized reduction in average threshold sensitivity (27.0 dB) and particular reduction in threshold sensitivity at the loci measured over the temporal lesion (23 dB).

To summarize, the patient presented with bilateral choroidal lesions whose nature was further characterized with the use of multimodal imaging. Specifically, the lesions in both eyes demonstrated ellipsoid zone disruption, suggesting an inflammatory etiology, with additional active Type-2 NV in the right eye. Serum studies for toxoplasmosis, tuberculosis, syphilis, HIV, and toxocariasis showed negative results. As a result, the patient was diagnosed presumptively with idiopathic MFC.

Upon initial presentation, the patient was treated with intravitreal bevacizumab in the right eye. Following a nonrevealing infectious workup, he was then started on oral prednisone 60 mg per day tapered over 1 month to treat the inflammatory lesions.

Both symptoms and visual acuity started to improve upon beginning the treatment. Visual acuity at 1 month was 20/40 in the right eye and 20/25 in the left eye. The patient received two additional intravitreal injections of bevacizumab to the right eye at monthly intervals. Visual acuities were 20/30 in the right eye and 20/20 in the left eye at 3 months.

At nine months after the initial presentation, the patient's visual acuity improved to 20/20 in the right eye and 20/25 in the left eye. Examination revealed no evidence of anterior chamber inflammation of either eye with stable superonasal vitritis of the right eye and without evidence of posterior chamber inflammation in the left eye. Ophthalmoscopic examination at this visit revealed a stable hypopigmented lesion in each eye, superior to the fovea in the right eye and temporal to the fovea in the left eye. Optical coherence tomography imaging revealed reestablishment of the ellipsoid zone in the right eye. The lesion in the left eye demonstrated resolution of subretinal hyperreflective material with an associated extrafoveal temporal scar (Figure 2). Interval reduction of choroidal thickness from baseline was also noted.

These findings correlated with artery occlusion imaging, demonstrating improvement in the number of cones visible within the MFC lesions (Figure 3). Cones were quantified using a semiautomated method. The lesion boundary was first defined using indocyanine green and scanning laser ophthalmoscopy images, and the mean of the center of each was designated as the center of the lesion. Regions of interest of 0.5° × 0.5° in size located 1.5°, 2.5°, and 3.5° away from the foveal center were demarcated both within and outside the lesion. The number of cones visible at each location was first marked using an automated algorithm⁴ and then positions were manually corrected. The number of visible cones within each ROI was then plotted over time and compared with unaffected regions of the same retina at equal eccentricities from the fovea. As demonstrated in Figure 4, the number of visible cones at each location increased between baseline imaging

Supported by NIH CORE Grant P30 EY08098 to the University of Pittsburgh Department of Ophthalmology, Departmental Startup Funds to EAR from the University of Pittsburgh Department of Ophthalmology, the Eye and Ear Foundation of Pittsburgh, and from an unrestricted grant from Research to Prevent Blindness, New York, NY. The sponsor or funding organization had no role in the design or conduct of this research.

K. B. Freund is a consultant for Bayer HealthCare, Roche/Genentech, Inc., Heidelberg Engineering, Novartis, Optovue, and Carl Zeiss Meditec and receives research support from Roche/Genentech, Inc. K. K. Dansingani is a consultant for Biogen. The remaining authors have any conflicting interests to disclose.

Reprint requests: Kunal K. Dansingani, MA, FRCOphth, UPMC Eye Center 203 Lothrop Street, 8th floor, Pittsburgh, PA 15213; e-mail: kkd@doctor.com.

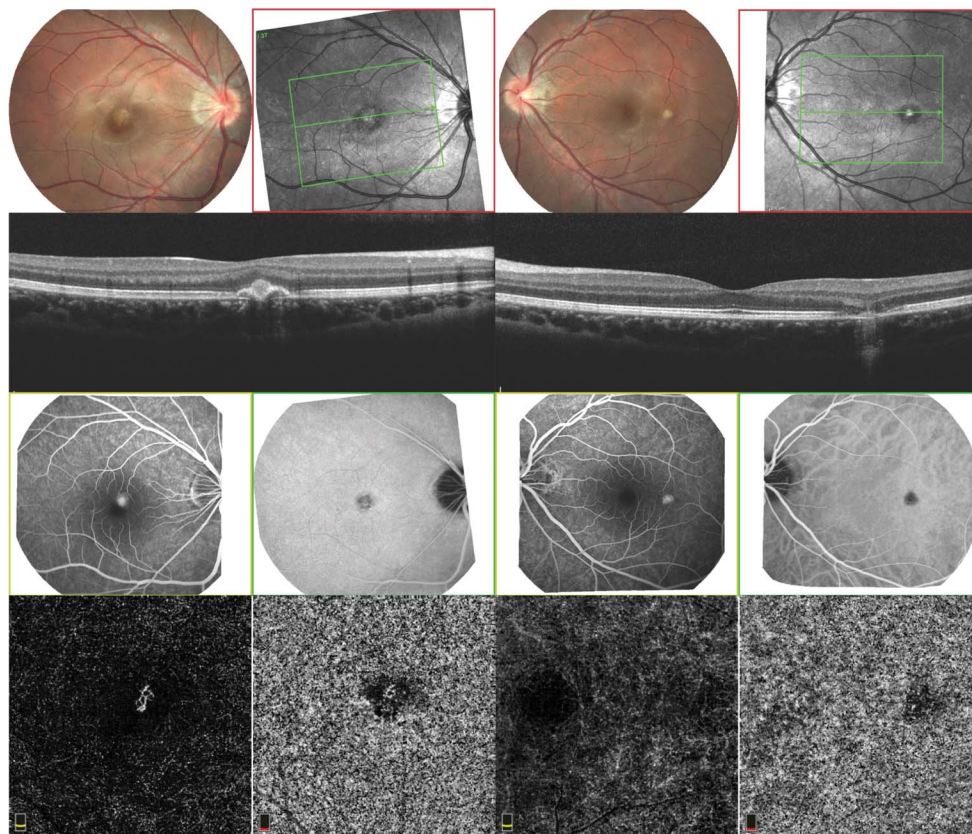


Fig. 1. Multimodal imaging of multifocal choroiditis at presentation. Fundus photography of the right eye is notable for hypopigmented lesion superior to the fovea, whereas the left eye has a hypopigmented lesion temporal to the fovea (top row). Spectral-domain OCT through the right eye lesion demonstrates a small, irregular, subfoveal, pigment epithelial detachment, subretinal hyperreflective material, and hypertransmission at the lesion. Optical coherence tomography of left eye demonstrates a small extrafoveal hypertransmissive lesion and minimal subretinal hyperreflective material (second row). Fluorescein angiography demonstrates early hyperfluorescence and late leakage in the right eye and midphase hyperfluorescence without leaking in the left eye (third row). Indocyanine green angiography in both eyes reveals hypofluorescence in the area of the lesions, attributable to choriocapillaris loss (third row). Optical coherence tomography angiography through the lesions demonstrates a flow signal in the right

eye but not in the left eye, at the level of the outer retinal bands (fourth row). Image brightness and contrast were optimized for display on screen and in print.

and repeat imaging at 6 and 10 months. Microperimetry was also repeated as shown in Figure 5; both eyes maintained steady fixation, and the average threshold sensitivity of each eye increased to 28.2 dB, which was normal compared with age-matched controls. Furthermore, there was additional localized improvement in sensitivity threshold in the region of the MFC lesion in the right eye from 15 dB on presentation to 24 dB at 12 months. The sensitivity threshold at the location of the lesion of the left eye remained stable at 23 dB.

Discussion

Multifocal choroiditis and/or punctate inner choroidopathy may be considered to define a continuous spectrum representing a progressive inflammatory chorioretinopathy. This disease can have a relapsing and remitting course with both inflammatory and neovascular sequelae.

Prior studies have localized pathologic alterations to the level of the sub-RPE and outer retina.¹ These anatomical changes are readily demonstrated with multimodal imaging. On OCT, active inflammatory lesions demonstrate focal or diffuse attenuation of the ellipsoid zone with partial photoreceptor loss at the edge of the lesion¹ and RPE discontinuity or elevation

as a result of deposition of homogenous hyperreflective material, associated with posterior hypertransmission. By contrast, inactive inflammatory lesions are characterized by re-establishment of the ellipsoid zone with possible localized absence of the RPE on OCT.⁴ Using fluorescein angiography, active inflammatory lesions are not readily visible in early frames but demonstrate late staining and leakage, whereas inactive inflammatory lesions do not leak.⁴ Secondary inflammatory NV can also be demonstrated using imaging. On fluorescein angiography, active macular NV is defined by early hyperfluorescence with late leakage, whereas inactive neovascular lesions demonstrate staining of scar tissue.⁴ Evidence of Type-2 NV on OCT includes heterogeneous hyperreflective material in the subretinal space representing inflammatory exudate and heme. These neovascular networks may also be visualized morphologically using OCT angiography.

To augment our understanding of this disease process, adaptive optics ophthalmoscopy of cone photoreceptors was performed at baseline and at seven and nine months of follow-up. We were particularly interested in highlighting areas where cone visibility

Downloaded from http://journals.lww.com/retinalcases by BNDM5epHKav1ZEoum1tQIN4+kLLHEZ9bsH04XM10h CymCX1AWnYQp/IQHD3I3D00dRy7TVSFI4C3VCAOAVpDDa8k2+Yab6H515KE= on 10/10/2023

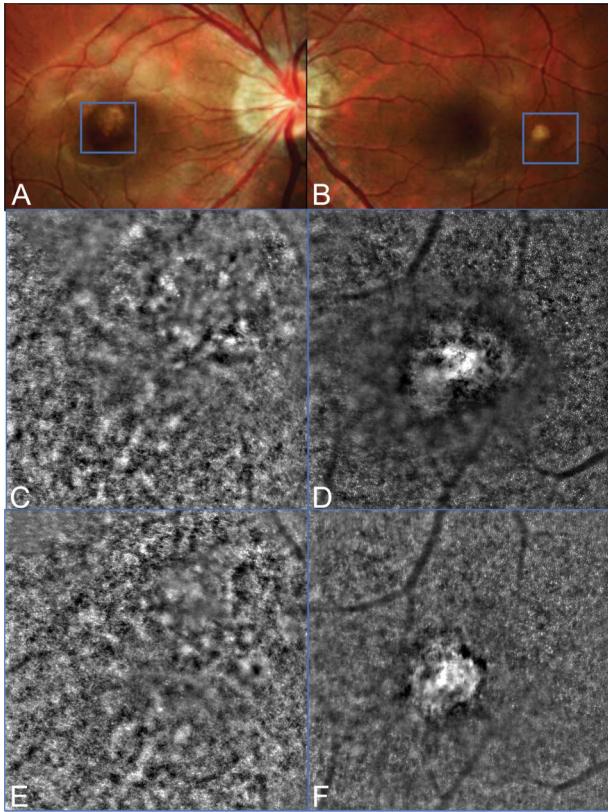


Fig. 2. Flood illumination adaptive optics of multifocal choroiditis lesions over time. The retinal areas imaged by adaptive optics ophthalmoscopy are indicated in by blue boxes (A and B). At initial presentation, there was reduced cone visibility at the location of the choroiditis lesions (C and D). At 9 months of follow-up, there is reorganization of photoreceptors and decreased size of the areas of disruption (E and F).

was lost and evaluating these regions in response to treatment and in comparison to standard clinical imaging. Visibility of the cone mosaic in FIAO may require an intact interdigitation zone and cone outer segments.⁵ Consequently, lesions that alter the structural integrity of these retinal layers demonstrate loss of outer segment reflectivity on OCT and loss of cone visibility using FIAO imaging.⁶ In the absence of a single, repeatable, automated metric to quantitatively evaluate the health of the cone mosaic, this study provides the first qualitative, longitudinal descriptions of the cone mosaic in MFC.

At baseline, the patient had bilateral inflammatory lesions with boundaries demarcated by loss of the interdigitation zone on OCT imaging. Adaptive optics imaging demonstrated loss of visible cones in both eyes localized to regions of active disease. Outside MFC lesions, the cone mosaic appeared normal within the macula of both eyes. After receiving appropriate therapy, reestablishment of the interdigitation zone on OCT in the right eye corresponded to improved visibility of the cone

mosaic on adaptive optics imaging, as demonstrated by the number of visibly cones increasing at each subsequent follow-up in the right eye. After nine months of follow-up, the left eye demonstrated continued loss of the interdigitation zone at the location of the original lesion with hypertransmission to the choroid. The boundaries of this lesion correlated with adaptive optics imaging demonstrating improved central hyperreflectivity with a halo of hyporefectivity and localized loss of the regular cone mosaic.

These adaptive optics imaging findings were consistent with prior reports that have identified structural alterations in the cone photoreceptors as a consequence of MFC. Specifically, prior studies have identified active lesions as focal hypointensities, whereas inactive lesions are characterized by a bright hyperreflective center with a circumferential hypointense halo.⁷ Loss of the cone mosaic on adaptive optics imaging may represent either loss of cones or structural alterations resulting in a reduction in scattering by the cones. The latter could be driven by either misalignment or shortening of the cone outer segments.⁶ Given that the cone density and regularity improved upon instituting therapy, our findings agree with those of prior studies that postulate that the reduction in cone density on presentation represents a reversible alteration in either the structure or directionality of the cone photoreceptor outer segments such that they are not detected by adaptive optics imaging.⁶ This is consistent with prior studies suggesting that eyes presenting with preserved outer nuclear layer, as in this case, have the potential to regain visual acuity and portend a more favorable prognosis.⁸ Although this study did not evaluate the presence of remaining inner segments using nonconfocal adaptive optics imaging, future work should consider the incorporation of such techniques in the study of MFC as those methods may reveal intact cone inner segments and could provide further insight into the photoreceptor alterations associated with MFC.

This article additionally offers the first demonstration of the functional consequences of alterations in cone photoreceptors on macular function in MFC. Macular integrity assessment microperimetry concurrently images the retina while measuring retinal sensitivity and can be repeated over time, allowing for correlation between microstructural changes and functional loss.⁶ Longitudinal microperimetry data can be compared on the bases of fixation stability, fixation location, macular sensitivity, and scotoma size.⁹

Microperimetry was obtained at baseline and at 1-year follow-up in our patient. Baseline microperimetry in the right eye showed stable fixation with an average macular sensitivity threshold (26.8 dB) that

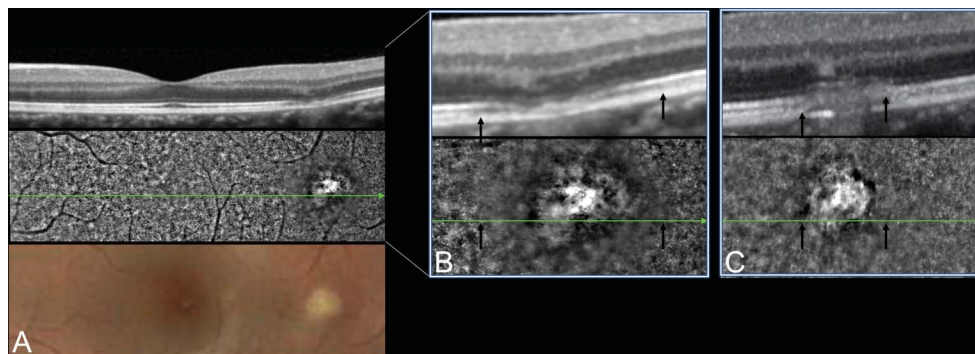


Fig. 3. Correlation of OCT and adaptive optics ophthalmoscopy of multifocal choroiditis lesion in the left eye. Spectral-domain OCT through the level of the lesion (green arrow) of the left eye with corresponding adaptive optics ophthalmoscopy and fundus photograph (left panel). The borders of photoreceptor disruption of the lesion correspond with interdigitation zone loss on OCT (black arrows) at presentation (middle panel) and at 9 months of follow-up

(right panel).

represented less than the fifth percentile compared with age-matched controls. Sensitivity was particularly reduced at the loci tested superiorly and superior-nasal to the fovea. Anatomically, these regions correlated with the focal area of NV. Similar findings were obtained at baseline in the left eye, which demonstrated stable central fixation but a generalized reduction in average macular sensitivity threshold (27.0 dB). At 1-year follow-up, the average macular sensitivity threshold improved in both eyes to within the range of normal compared with age-matched controls. Fixation remained grossly stable in both eyes, although the slight reduction in fixation stability in the left eye at 1-year follow-up may represent testing fatigue. There were no scotomata in either eye at baseline or at 1-year follow-up.

In addition to longitudinal comparisons between active and inactive disease, the case also provides comparison between the effects of inflammatory and neovascular consequences of MFC on structure and function. Optical coherence tomography and fluorescein angiography demonstrated that the parafoveal lesion in the right eye had both inflammatory and secondary neovascular components on initial presentation, whereas the lesion of the left eye temporal to the fovea was primarily inflammatory.

At presentation, adaptive optics imaging demonstrated that both the active secondary neovascular lesion in the right eye and the inflammatory lesion in the left eye disrupted the visibility of the cone mosaic. At the location of both lesions, there was central loss of the cone mosaic with a rim of normal architecture

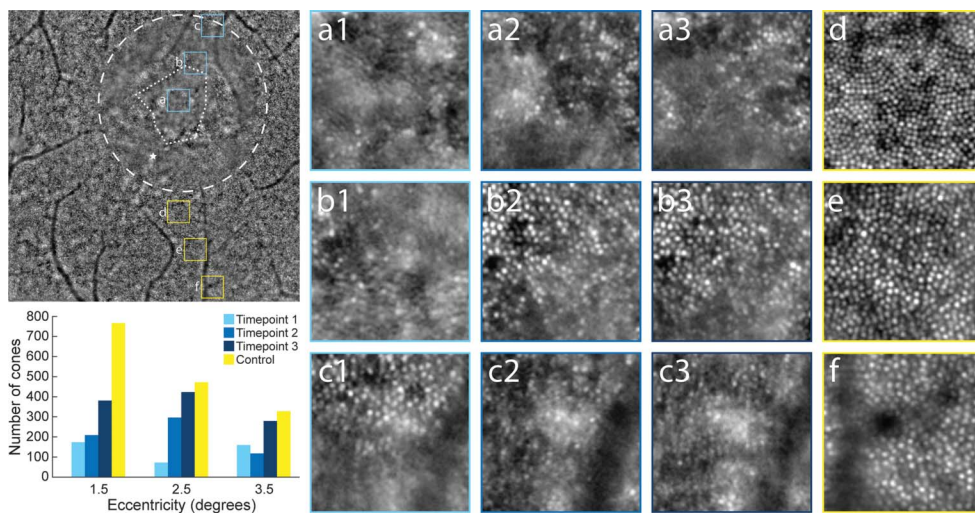


Fig. 4. Cone recovery quantification across the lesion area in the right eye. The lesion boundary was defined on both the indocyanine green angiogram (dotted polygon) and adaptive optics (artery occlusion) images (dashed ellipse). The lesion center was defined as the averaged center of the lesion as defined from each and was marked with a star. Regions of interest of $0.5^\circ \times 0.5^\circ$ in size were marked at locations 1.5° , 2.5° , and 3.5° , both within the lesion (A–C) and outside the lesion (D–F). The locations are denoted at the upper left montage images. a1–c1 are from the initial time of artery occlusion imaging (April

19, 2018), a2–c2 are from approximately 5 months later (November 1, 2018), and a3–c3 are from the final imaging session that occurred 9 months from presentation (January 31, 2019). Control points are those obtained during the initial imaging session. Plot at lower left shows that the number of visible cones steadily increased at each subsequent session at locations a and b. Interestingly, the recovery of cone visibility near location (A) was near a location where sensitivity increased substantially between imaging sessions (see Fig. 4). However, location c appeared to be at the boundary of the lesion. As a result, the image quality decreased at the second time point relative to the first, which may explain why the visible cone count decreased at the second time point but subsequently increased at the third time point. Of note, location c and its control location (F) each had a blood vessel shadow within the regions of interest that partially obstructed the cones; the area filled with the vessel shadow was nearly identical in each (13.8% of the pixels in the control location vs. 12.7% of the pixels in the lesion location).

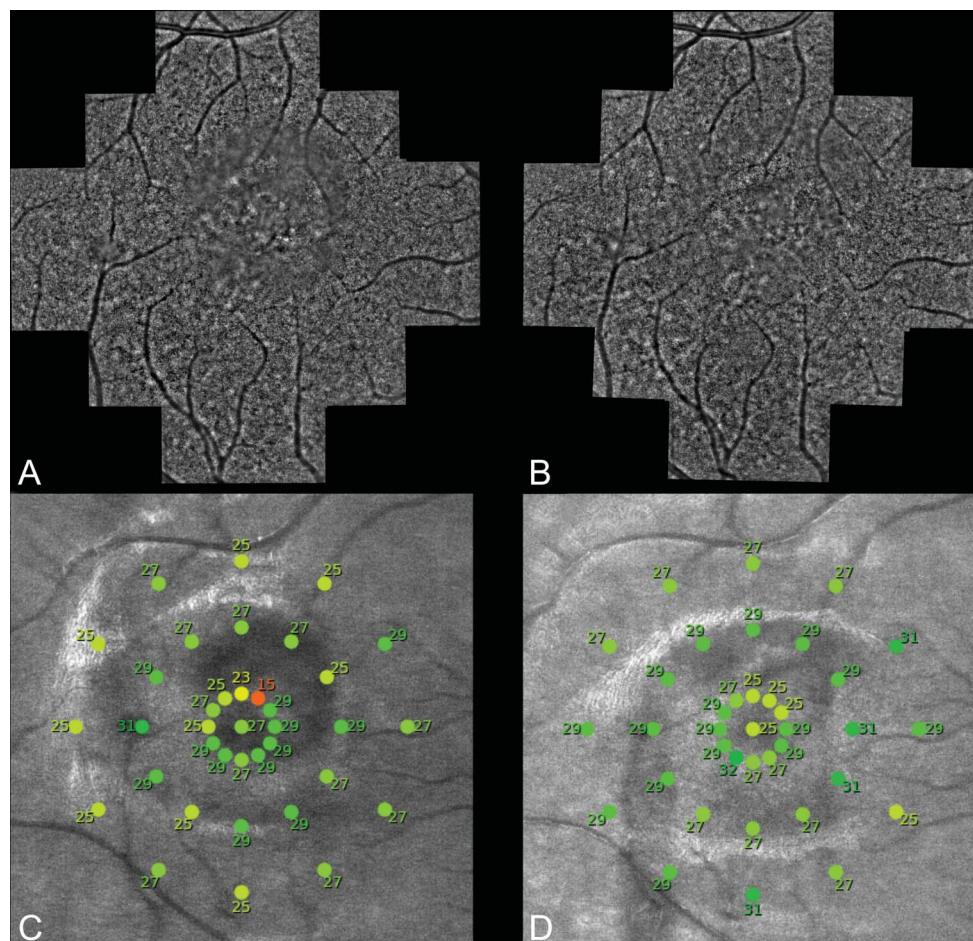


Fig. 5. Corresponding changes in adaptive optics ophthalmoscopy and microperimetry of foveal multifocal choroiditis lesion in the right eye. Montage adaptive optics ophthalmoscopy images of the posterior pole of the right eye at presentation (A) and at 9 months follow-up (B), demonstrating reorganizing of photoreceptor and decreased size of photoreceptor disruption over time. Corresponding macular integrity assessment microperimetry images demonstrated decreased sensitivity and eccentric fixation at presentation (C), which normalizes by 9-month follow-up (D).

surrounded by a second region of where cone photoreceptor visibility was lost. The loss of cone signal in adaptive optics images appeared more profound at the inflammatory lesion of the left eye than at the neovascular lesion in the right eye. With appropriate therapy, the neovascular lesion of the right eye became inactive and the inflammatory lesion in the left eye regressed in size, with residual scar formation. As a result, at 1 year from presentation, adaptive optics demonstrated that in both eyes, the area of preserved cone density and regularity was larger than at initial presentation. However, consistent with OCT evidence of improved integrity of the interdigitation zone at the location of the lesion in the right eye, the cone mosaic was consistently better visualized in the right eye than at the lesion of the left eye, which continued to demonstrate interdigitation zone loss on OCT at 1 year. Furthermore, microperimetry data obtained from both eyes demonstrated that the neovascular lesion in the right eye caused a greater decrease in localized threshold sensitivity than the inflammatory lesion in the left eye on initial presentation. However, the threshold sensitivity at the location of the neovascular

lesion in the right eye improved with both intravitreal bevacizumab and systemic prednisone. By contrast, the threshold sensitivity at the location of the purely inflammatory lesion in the left eye demonstrated minimal change after systemic prednisone therapy, indicating that there may have been some continued low-grade disease activity. Together, these findings suggest that the inflammatory lesions of MFC may cause greater structural and functional alterations in the interdigitation zone than do the neovascular lesions. This is important because these effects may not be captured by measures of visual acuity alone if the causative lesion is outside of the fovea, as is the case in our patient.

In this article, we demonstrate that adaptive optics imaging can be used to provide further information regarding the nature and activity of inflammatory choroidal lesions, which correlate to functional changes on microperimetry. Specifically, active lesions were characterized by the loss of outer segment reflectivity and loss of cone mosaic visibility with an associated reduction in foveal sensitivity on microperimetry. Fortunately, both structural and functional

alterations were responsive to anti-inflammatory and anti-vascular endothelial growth factor therapy, as reestablishment of the ellipsoid and interdigitation zones and increased cone visibility correlated with improved foveal sensitivity on microperimetry as the lesions became quiescent. However, in this case study, these improvements were greater in neovascular lesions than the purely inflammatory, nonneovascular lesions. Therefore, both adaptive optics imaging and microperimetry may be used as adjunctive biomarkers of disease type and activity in MFC. In summary, we demonstrate the value of a longitudinal multimodal and multiscale imaging approach to diagnosing, characterizing, and following the course of idiopathic MFC.

Key words: adaptive optics, microperimetry, multifocal choroiditis, punctate inner choroidopathy, imaging.

References

1. Spaide RF, Goldberg N, Freund KB. Redefining multifocal choroiditis and panuveitis and punctate inner choroidopathy through multimodal imaging. *Retina* 2013;33:1315–1324.
2. Olsen TW, Capone A, Sternberg P, et al. Subfoveal choroidal neovascularization in punctate inner choroidopathy. Surgical management and pathologic findings. *Ophthalmology* 1996;103:2061–2069.
3. Tavallali A, Yannuzzi LA. Idiopathic multifocal choroiditis. *J Ophthalmic Vis Res* 2016;11:429–432.
4. Li KY, Roorda A. Automated identification of cone photoreceptors in adaptive optics retinal images. *J Opt Soc Am A* 2007;24:1358–1363.
5. Litts KM, Cooper RF, Duncan JL, Carrol J. Photoreceptor-based biomarkers in AOSLO retinal imaging. *Invest Ophthalmol Vis Sci* 2017;58:BIO255–BIO267.
6. Jacob J, Paques M, Krivosic V, et al. Meaning of visualizing retinal cone mosaic on adaptive optics images. *Am J Ophthalmol* 2015;159:118–123.
7. Agarwal A, Soliman MK, Hanout M. Adaptive optics imaging of retinal photoreceptors overlying lesions in white dot syndrome and its functional correlation. *Am J Ophthalmol* 2015;160:806–816.
8. Kaden TR, Gattoussi S, Dolz-Marco, et al. The nature and frequency of outer retinal disruption in idiopathic multifocal choroiditis associated with persistent fundus hyperautofluorescence. *Ophthalmic Surg Lasers Imaging Retina* 2019;50:675–683.
9. Hong IH, Park SP. Quantitative physiological measurements to evaluate the response of anti-vascular endothelial growth factor treatment in patients with neovascular diseases. *Indian J Ophthalmol* 2017;65:559–568.